Chalcogenide Letters Vol. 19, No. 10, October 2022, p. 715 - 723

Effect of thulium oxide on structural, refractive index, and optical band gap of bismuth-boro-tellurite glass system

R. Falihan[a,b], L. Hasnimulyati[c], N. A. Abdul-Manaf[b], W. Y. W. Yusoff[b], A. H. Azmi[b], A. Azuraida[b,*]
[a]*Faculty of Defence Science and Technology, National Defence University of Malaysia, Sungai Besi Camp, 57000 Kuala Lumpur, Malaysia*
[b]*Centre for Defence Foundation Studies, Universiti Pertahanan Nasional Malaysia, 57000 Kuala Lumpur, Malaysia*
[c]*Faculty of Applied Sciences, Universiti Teknologi Mara Pahang, 26400 Jengka, Pahang, Malaysia*

The bismuth-boro-tellurite glass has been chosen by various analysts from all around the world due to its advantages and ability the improvement of glass technologies. This paper aims to study the structural and optical properties of the bismuth-boro-tellurite glass system with different amounts of thulium oxide as a glass dopant. Four glass sample from chemical composition of $[(B_2O_3)_{0.25}\ (TeO_2)_{0.75}]_{0.75}\ [(Bi_2O_3)_{0.25}]_{1-x}\ [Tm_2O_3]_x$ (x = 0.000, 0.005, 0.010, and 0.015 mol%) were prepared by melt-quenching method with suitable melting and quenching temperature. The Ultraviolet-Visible Spectroscopy (UV-Vis) was used for recording their optical absorption spectra. These optical absorption spectra were used to determine the optical band gap energy, refractive index, and polarizability of all glass samples. While the structural changes are observed using X-ray diffractometer (XRD) and Fourier Transform Infrared Spectroscopy (FTIR).

(Received June 21, 2022; Accepted October 13, 2022)

Keywords: Tellurite glass, Thulium, Refractive index, Bandgap, Urbach energy

1. Introduction

Boro (B_2O_3) and tellurite (TeO_2)-based glasses have been widely studied and well known because of their distinct physical properties and industrial importance in processing glasses with desirable optical properties [1]. Boro-tellurite based glass has a low melting point, non-hygroscopic, high density, high refractive index, and good transparency in the far-infrared region [2]. Furthermore, these glasses are highly stable against devitrification, non-toxic, and are resistant to moisture for long periods as compared with those conventional glasses [3].

Bismuth is a quite unique material among heavy metals, and it can be considered a harmless, non-toxic, and non-carcinogenic material. It is valuable in electronics application, ceramic production, and a good element for "warm" superconductors because of the high polarizability of Bi^{3+} cations [4]. Because of the small field strength of Bi^{3+} ions, bismuth oxide cannot be considered a network former, however, in combination with B_2O_3, glass formation is possible in a relatively large composition range [5]. Bismuth oxide occupies both network-forming and network-modifying positions [6]. The addition of bismuth oxide in borate glass is of great interest in optoelectronic devices due to its low melting temperature (600–900 ºC), extensive glass formation range, high refractive index ranging, and high physical and chemical stability, [4].

Rare-earth ions have been intensively investigated in the glass system concerning their physical and chemical composition in the glass network which determines the structure and nature of glass. It also includes optical properties. Since 1975, the use of rare earth material as a dopant for glass series has greatly developed. The tellurite-based glasses with enough rare earth elements emerged in several situations [2,7]. However, tellurite glass only can be formed with the addition of alkali, alkaline earth, and transitional metal oxides or other glass formers [8]. The development

* Corresponding author: azuraida@upnm.edu.my
https://doi.org/10.15251/CL.2022.1910.715

of rare-earth ions doped glasses is right on track due to their outstanding potential application such as in optical, semiconductors, telecommunication, x-ray imaging, sensors, lasers, etc. [2,9].

Thulium (Tm^{3+}) is generally considered to be one of the strongest active ions in the world [10]. The chemical structure of Tm_2O_3 which was studied in the present investigation has several applications. In the previous study, thulium oxide was added to the glass system to enhance its optical properties. Tm_2O_3 is a rare earth element, and its properties are dependent on the nature of the precursor used for its preparation as well as the pre-treatment conditions, which determine its basicity [11]. Research done by [12] was reported that Tm^{3+} doped tellurite glasses have a great potential to be used as an efficient optical fiber amplifier in the 1.47 μm region. Meanwhile, according to [13] Tm^{3+} ions occupied the network sites as modifying oxides and stabilizing non-bridging oxygens (NBOs) bonds. In this research, more data will be provided on the advantages of bismuth-boro-tellurite glass doped with thulium oxide in terms of its structural and optical properties. It is expected that the addition of a small amount of thulium oxide in the glass system will enhance the optical properties such as the optical band gap, refractive index, and molar polarizability.

2. Experimental arrangement

The glass system with chemical composition of $[(B_2O_3)_{0.25}\ (TeO_2)_{0.75}]_{0.75}\ [(Bi_2O_3)_{0.25}]_{1-x}\ [Tm_2O_3]_x$ (where x = 0.000, 0.005, 0.010 and 0.015 mol%) successfully prepared by melt-quenching technique. Each glass batch were prepared from certified reagent grades of TeO_2 (99.95% purity), B_2O_3 (97.5%), Bi_2O_3 (99.975% purity), and Tm_2O_3 (99.99%) were of commercial origin which manufactured and supplier by Alfa Aesar. The chemicals were firstly mixed and grinded repeatedly for 30 minutes in an alumina crucible until become excessively a fine powder substance before being heated at 1000 ºC for 1 hour. After the batch is completely melted, the molten was poured onto the preheated stainless-steel plate and annealed at 400 ºC for 1 hour before being allowed to cool down to room temperature. The amorphous nature of all glass samples was checked using X-ray Diffraction (XRD) while the chemical bonding that exists was recorded by Fourier Transform Infrared Spectroscopy (FTIR) in the range number 650-4000 cm^{-1}.

The glass density was determined using Electronic Densimeter: MD-300S that operated based on the Archimedes principle with distilled water as the immersion fluid. The value then can be calculated using the following formula:

$$\rho = \frac{m_a}{m_a - m_w}\rho_w \tag{1}$$

where ρ is the density of the sample, ρ_w is the density of water, m_a is the mass of sample in the air, and m_w is the mass of a sample in water. After that, molar volume, V_m can be calculated using the equation:

$$V_m = \frac{M}{\rho} \tag{2}$$

where M is the total molecular weight [14].

The optical absorption coefficient $\alpha(\omega)$ for each sample, was calculated at different photon energies by using the relation $\alpha(\omega) = 2.303\ A/d$, where A is absorbance and 'd' is the thickness of the samples [15]. The optical energy band gap (E_{opt}) was determined by the interpolation of the linear region of plotting the $\hbar\omega$ axis at $(\alpha\hbar\omega)^2=0$ for direct allowed transitions [16].

Furthermore, another optical parameter called Urbach energy has been obtained from absorption spectra. It is derived by evaluating the reciprocal of slope in the graph of the natural logarithm of $\alpha(\omega)$ as a function of photon energy ($\hbar\omega$), according to the equation from the Urbach rule:

$$\alpha(\omega) = \alpha_0 exp\left(\frac{\hbar\omega}{\Delta E}\right) \tag{3}$$

where α_0 is constant and ΔE is the Urbach energy. Meanwhile the refractive index of the glass samples was calculated using the following relations proposed by [17]:

$$\frac{n^2-1}{n^2+2} = 1 - \sqrt{\frac{E_{opt}}{20}} \quad (4)$$

where n is the refractive index and E_{opt} is the optical band gap value for a direct transition of the glass samples. Besides, the molar refraction and molar polarizability can be calculated by using the equation:

$$\left(\frac{n^2-1}{n^2+2}\right) V_m = R_M \quad (5)$$

$$R_M = \frac{4}{3}\pi N_A a_m \quad (6)$$

where R_M is the molar refraction, n is the refractive index, V_m is the molar volume, N_A is Avogadro constant, and a_m is the molar polarizability of the glass.

3. Result and discussion

XRD pattern for the prepared glass sample is shown in Fig. 1. The structure of glass after adding the Tm_2O_3 inside the glass system is influential to the properties. It can be seen that the pattern in Fig. 1 indicates the existence of usually short-range structural distortion of broad main peaks at (2θ = 28°), which features an amorphous nature [18-19]. However, a small peak was produced at 2θ = 32°, which shows that the glass sample started to form into partial crystallinity [20-21]. These peaks appear with a slightly increasing intensity when the thulium amount increased to 0.015 mol%. The broad peak at 28° is suggested to be due to the formation of the α-TeO_2 phase while the crystalline peaks at 32° are suggested due to the existence of the γ-TeO_2 phase [20]. According to these findings, undefined Tm_2O_3 crystals exist and still have a glassy appearance. The structural change only plays a minor role in the concentration borate glass system to investigate the amorphous nature. Each pattern that has a hump was increased in intensity with the addition of thulium oxide [22].

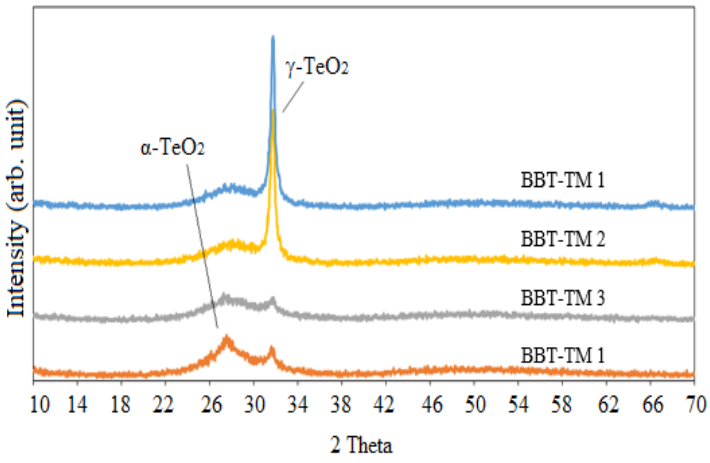

Fig. 1. XRD spectra of the present glasses.

Table 1 shows the density and molar volume value of all glass samples, and it is also plotted on the graph in Fig. 2. With the addition of Tm_2O_3 up to 0.015 mol fraction, the density of the glass system increased from 6.066 g/cm^3 to 6.181 g/cm^3 while the molar volume decreased from 36.271 cm^3/mol to 35.887 cm^3/mol. The pattern of this result follows the relationship between density and molar volume as shown in Equation (2), which is the molar volume and

density are inversely proportional to each other. The increase in density might be attributed to the higher molecular weight of thulium oxide when compared to other chemical oxides [20]. The addition of thulium to the glass network increased the total molecular weight of the material.

Table 1. Sample code, molar fraction of Tm_2O_3, density (ρ), and molar volume (V_m) of the glass samples.

Sample Code	Mol fraction	ρ (g/cm^3)	V_m (cm^3/mol)
BBT-TM 1	0.000	6.066	36.271
BBT-TM 2	0.005	6.075	36.239
BBT-TM 3	0.010	6.114	36.144
BBT-TM 4	0.015	6.181	35.887

The density of the glass was also increased since density is directly proportional to molar mass [23]. Furthermore, producing a compact glass Tm ion allows the lower ionic radii to fill the interstitial gaps of the glass network [24]. In terms of molar volume, the Tm ion leads to contraction and consequent reduction in molar volume that is related to a decrease in molar volume because of the difference in ionic sizes [20]. In the previous study, decreases in the molar volume might be attributed to a decrease in bond length whereas the number of free volumes inside the glass network may reduce due to the higher dopant atom coordination number of Tm_2O_3 [22]. This feature might be related to a decrease in the number of oxygen atoms in a chemical unit's structure.

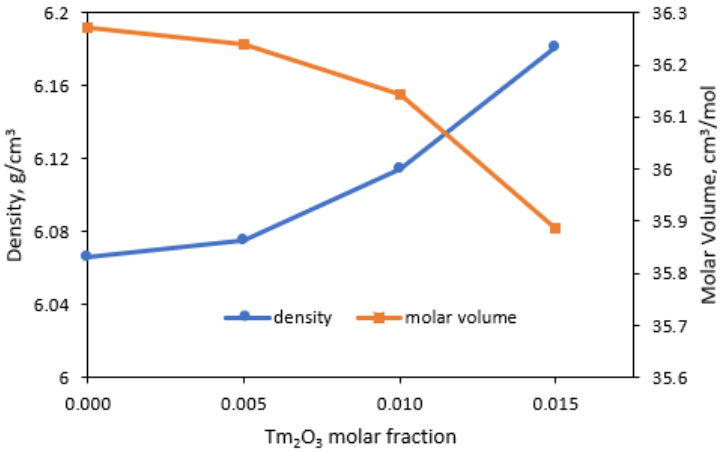

Fig. 2. Density and molar volume of $[(B_2O_3)_{0.25}\ (TeO_2)_{0.75}]_{0.75}\ [(Bi_2O_3)_{0.25}]_{1-x}\ [Tm_2O_3]_x$ glass system.

The FTIR spectra of present glasses are shown in Fig. 3. The FTIR spectra of thulium doped bismuth boro-tellurite glass are measured in the range of wavenumber between 650 cm^{-1} and 4000 cm^{-1}. From Fig. 3, it can be seen that there is observation of major absorption bands that are in 650-780 cm^{-1}, 809 cm^{-1}, 820-906 cm^{-1}, 911-1111 cm^{-1}, 1200-1500 cm^{-1}, 2993-3003 cm^{-1}, and 3618-3748 cm^{-1}. These assignments of infrared transmission bands for $[(B_2O_3)_{0.25}\ (TeO_2)_{0.75}]_{0.75}\ [(Bi_2O_3)_{0.25}]_{1-x}\ [Tm_2O_3]_x$ are also given in Table 2. The band at 650-780 cm^{-1} is assigned for TeO_3 trigonal pyramidal and TeO_4 trigonal bipyramidal. The size of the peaks that correspond to the amount of TeO_4 increases along with the increases in Tm^{3+} concentration [25-26]. The characteristic of pure borate B_2O_3 glass was centered at 806 cm^{-1} which is the characteristic peak of the boroxly ring overlapping with the Te-O bond with non-bridging oxygens [27].

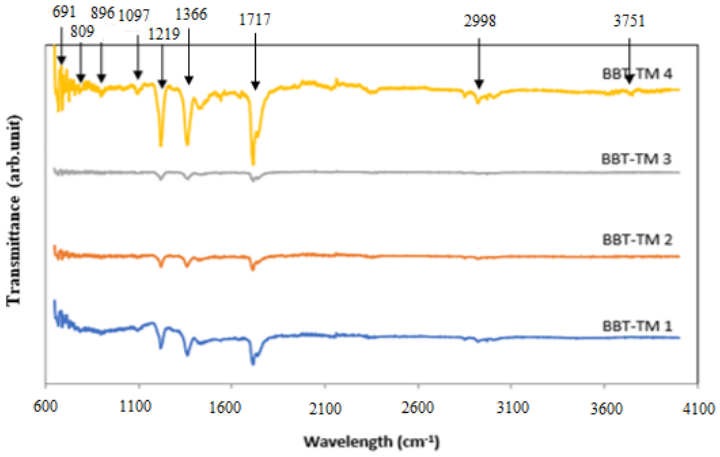

Fig. 3. FTIR spectra of present glass.

However, the absence of an absorption band at 820-906 cm^{-1} in the previous glass system shows that there are no boroxyl ring forms in the structure of glasses, which ultimately contains BO_3 and BO_4 groups [28-29]. Stretching modes of $[BO_4]^-$ tetrahedral boron coordination is responsible for the peaks at 911–1110 cm^{-1} [25]. At lower Tm_2O_3 concentrations, this peak is unidentifiable. However, the peak can be detectible for glass with 0.010 mol % of thulium concentration. At 1200–1800 cm^{-1}, the peak for $[BO_3]^0$ appears [30]. The bridging oxygen is formed which is validated by the creation of TeO_4 and BO_4 structural units [31], thus it increases the Tm^{3+} due to the addition of Tm_2O_3 into the glass system as it made the peak become shallower [32]. Meanwhile, BO_4 structural units increase while the BO_3 triangular borons increase [30]. According to [33], the characteristics of the hydrogen bond H-O were related to the band at 2993-3003 cm^{-1} in the glass system. The OH appears because of the effect of a dry atmosphere. The area of the -OH absorption band and the vibration of strong OH groups are reduced by bonded with hydrogen (H-OH) [10]. Moreover, the absorption bands in the 3618-3748 cm^{-1} range were caused by the fundamental stretching of molecule water groups, OH [34]. While the band observed at 3751 cm^{-1} is assigned to the weakly bonded hydrogen (H-OH) that is reduced to the free -OH groups [35]. The absence of a Tm-O bond that is undetectable by the equipment could be attributed to the low concentration of Tm_2O_3 [36].

Table 2. Assignment of infrared transmission bands for present glass.

Wavenumber (cm^{-1})	**Assignment**	**Refs.**
650-780 cm^{-1}	Te-O bonds stretching vibrations in TeO_4 units	[25], [26]
809 cm^{-1}	The peak of boroxyl ring	[27]
820-906 cm^{-1}	Stretching vibrations of the B-O bonds in BO4 units from diborate groups	[28], [29]
911-1110 cm^{-1}	B –O stretching vibrations in BO4 tetrahedral boron	[25]
1200-1800 cm^{-1}	Stretching vibrations of the B-O bonds of BO_3 from different types of borate groups	[30], [32]
2993-3003 cm^{-1}	The characteristic of the hydrogen bond H-O groups strongly in the glasses	[33]
3618-3748 cm^{-1}	stretching of molecule water groups, OH	[34]

Table 3. Optical band gap E_{opt}, Urbach Energy, ΔE, refractive index, n, molar refraction, R_m and molar polarizability, a_m of present glasses.

Sample Code	E_{opt} (eV)	ΔE (eV)	n	R_m	a_m (Å^3)
BBT-TM 1	3.17	0.170	2.402	22.200	8.800
BBT-TM 2	3.16	0.189	2.405	22.274	8.830
BBT-TM 3	3.09	0.211	2.439	22.500	8.921
BBT-TM 4	3.15	0.213	2.413	22.128	8.772

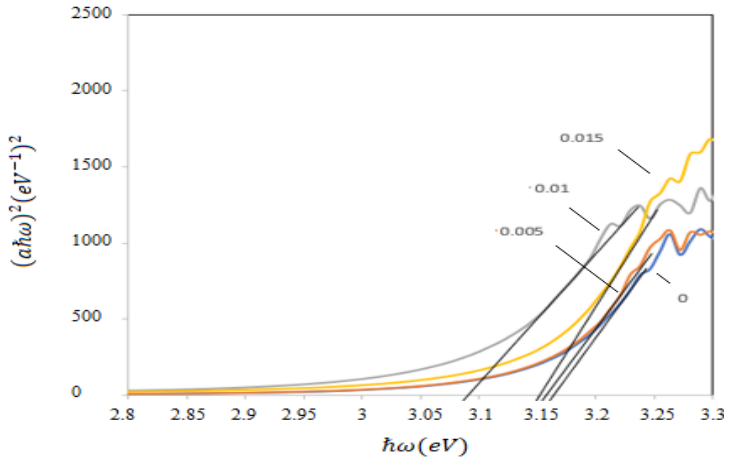

Fig. 4. Plot of $(a\hbar\omega)^2$ vs ħω for $[(B_2O_3)_{0.25}\ (TeO_2)_{0.75}]_{0.75}\ [(Bi_2O_3)_{0.25}]_{1-x}\ [Tm_2O_3]_x$ glass system.

The variations of the optical band gap (direct allowed) are measured as shown in Fig. 4 and also presented in Table 3. The variation of the optical bandgap for present glasses was found with the different amounts of thulium oxide, Tm_2O_3. Due to the vibration in the glass system, there might be a change in the amount of bridging oxygens (BOs) and non-bridging oxygens (NBOs). The value of the optical bandgap is decreased with the addition of dopant amount might be due to the increasing amount of non-bridging oxygens accompanied by electrons that are less bounded [37].

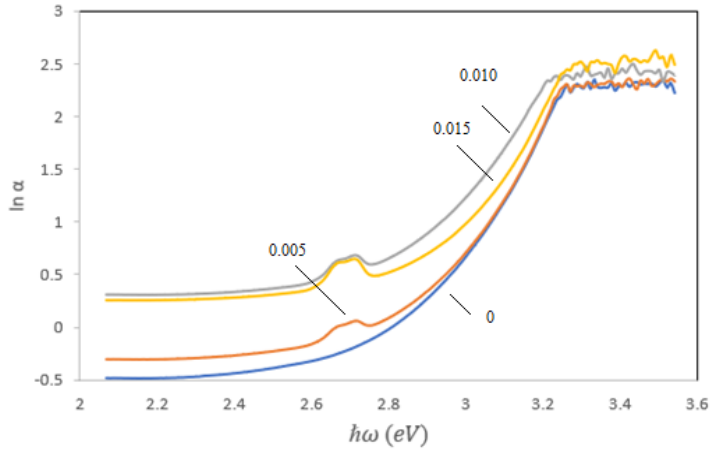

Fig. 5. Plot of ln α vs ħω for $[(B_2O_3)_{0.25}\ (TeO_2)_{0.75}]_{0.75}\ [(Bi_2O_3)_{0.25}]_{1-x}\ [Tm_2O_3]_x$ glass system.

As a result, electrons more easily transition from the valence band to the conduction band [38]. Furthermore, the presence of trivalent electrons Tm^{3+} ions increased the number of free

electrons in the glass network. These induced electrons to condense in low energy levels, contributing to E_{opt} decline [39]. Besides, the formation of more defects in the network might be a contributing factor to this trend. The slight increment of thulium in the glass system causes the rearrangement of atoms in the structure, causing TeO_3 to convert into TeO_4 structural units [40].

The Urbach energy contains information on defects and effects that reduce the long-range order in the glass network [25]. The reciprocal of the slope of the linear section (in the lower photon energy) in the graph of ln(a) against photon energy, as shown in Fig. 5, was used to calculate the Urbach energy for the present glasses. In the present study, the trend of Urbach energy data was found to increase as the increases in amount of dopant (Tm_2O_3). The increasing value of Urbach energy from 0.17 to 0.213 eV for concentration of dopant from 0.005 to 0.015 molar fraction indicates that the vitreous network's fragility is increasing. The increase of defect in the glass network makes the glass structure becomes less stable, more dislocated and leads to decreases in glass compactness [41]. The transformation of TeO_4 to TeO_3 and BO_4 to BO_3 units could be contributing to the increase in Urbach energy, which is attributed to the weak connection and the presence of more non-bridging oxygens (NBOs) [31]. Furthermore, the transformation of structural units has a higher degree of connectivity and thus increased glass defects. A previous study shows that the Urbach energy values were increased from 0.14 to 0.31 eV with the addition of thulium oxide. Due to linear polarizability, the thulium (Tm^{3+}) ions have an incomplete outer electronic configuration. TeO_4 units at a known equatorial position, occupied by a lone pair of electrons, are converted to TeO_3 units and non-bridging oxygens (NBOs) by Tm^{3+} ions. The non-bridging oxygens (NBOs) were quickly excited with lower energy and a higher number of polarizability than bridging oxygens (BOs). The number of free electrons in the outer shell of oxygen atoms was reverted by bridging oxygens (BOs) [42].

The refractive index of a glass is the most important property in optical which is associated with the polarizability and density of the ionic particle of the glass matrix [43]. The ratio of the velocity of light in a vacuum to the velocity of light in a specific medium is defined as the refractive index. Because the velocity of light is transmitted slower in high-density compounds, the refractive index of a denser material should be greater than that of a lower-density material. The data of refractive index, n, molar refraction, R_m and molar polarizability, a_m are listed in Table 3. Based on the present result, the refractive index for thulium oxide doped borotellurite glass generally increases from 2.402 to 2.413. The value of the refractive index increased because of the direct association between the refractive index and density [2]. In addition, molar refraction and polarizability are strongly related to the refractive index. The high polarizability of thulium ions will increase the molar polarizability, together with increasing the molar refraction and refractive index. In addition, non-bridging oxygens (NBOs) are more polarizability than bridging oxygens (BOs). This also will affect the increase of the refractive index [44].

4. Conclusion

A series of quaternary tellurite glass system with the composition of $[(B_2O_3)_{0.25}(TeO_2)_{0.75}]_{0.75}$ $[(Bi_2O_3)_{0.25}]_{1-x}$ $[Tm_2O_3]_x$ (where x = 0.000, 0.005, 0.010 and 0.015 mol %) were successfully prepared by melt-quenching technique. The addition of thulium oxide Tm_2O_3 to the bismuth-boro-tellurite glass system was found to increase density and decreased the molar volume of the glass. Analysis of the XRD pattern shows a broad peak which confirmed the amorphous nature, but the glass system started to form into partial crystallinity after the addition of 0.01 mol % Tm_2O_3. Analysis of FTIR spectra shows that there is an increase of amount non-bridging oxygens when increasing the Thulium oxide up to 0.015 mol %. Analysis of UV-Vis's spectra shows that the optical band gap energy value, E_{opt} was found to be increased with the increase of thulium oxide concentration, which is due to the presence of non-bridging oxygens. The increased band gap is explained by the expansion of the glass network.

Acknowledgments

The authors appreciate the financial support from the Universiti Pertahanan Nasional Malaysia, under GPJP, grant no. UPNM/2022/GPJP/SG/3.

References

[1] A. S. Abouhaswa, Y. S. Rammah, S. E. Ibrahim, and A. A. El-Hamalawy, Journal of Non-Crystalline Solid, 494, 59-65 (2018); https://doi.org/10.1016/j.jnoncrysol.2018.04.051

[2] K. Azman, H. Azhan, S. Y. S. Syamsyir, A. Mardhiah, and M. R. S. Nasuha, Material Science Forum, 846, 193-198 (2016); https://doi.org/10.4028/www.scientific.net/MSF.846.193

[3] S. P. H. S. Hashim, H. A. A. Sidek, M. K. Halimah, K. A. Matori, and W. M. D. W. Yusoff, Solid State Sciene and Technology, 19, 342-347 (2011)

[4] A. Azuraida, M. K. Halimah, A. A. Sidek, C. A. C. Azurahanim, S. M. Iskandar, M. Ishak, A. Nurazlin, Chalcogenide Letter, 12, 497-503 (2015)

[5] L. Baia, R. Stefan, W. Kiefer, J. Popp, and S. Simon, Journal of Non-Crystalline Solids, 303(3), 379-386 (2002); https://doi.org/10.1016/S0022-3093(02)01042-6

[6] S. Damodaraiah, V. Reddy Prasad, and Y. C. Ratnakaram, Spectrochimica Acta - Part A: Molecular and Biomolecular Spectroscopy, 181, 264-269 (2017); https://doi.org/10.1016/j.saa.2017.03.060

[7] Y. S. M. Alajerami, S. Hashim, W. M. S. Wan Hassan, A. Termizi Ramli, and A. Kasim, Physica B: Condensed Matter, 407(13), 2398-2403 (2012); https://doi.org/10.1016/j.physb.2012.03.033

[8] N. S. Sabri, A. K. Yahya, R. Abd-Shukor, and M. K. Talari, Journal of Non-Crystalline Solids, 444, 55-63 (2016); https://doi.org/10.1016/j.jnoncrysol.2016.04.038

[9] A. Malge, T. Sankarappa, T. Sujatha, P. Abdul Azeem, G. B. Devidas, and S. Kori, Materials Today: Proceedings, 26(9), 1960-1963 (2019); https://doi.org/10.1016/j.matpr.2020.02.428

[10] H. Gebavi, D. Milanese, G. Liao, Q. Chen, M. Ferraris, M. Ivanda, O. Gamulin, S. Taccheo, Journal of Non-Crystalline Solids, 355, 548-555 (2009); https://doi.org/10.1016/j.jnoncrysol.2009.01.016

[11] G. A. M. Hussein, G. A. H. Mekhemer, and B. A. A. Balboul, Physical Chemistry Chemical Physics, 2(9), 2033-2038 (2000); https://doi.org/10.1039/b000220h

[12] D. H. Cho, Y. G. Choi, and K. H. Kim, Chemical Physics Letters, 322, 263-266 (2000); https://doi.org/10.1016/S0009-2614(00)00408-5

[13] Y. Tian, R. Xu, L. Zhang, L. Hu, and J. Zhang, Journal of Applied Physics, 108(8), (2010); https://doi.org/10.1063/1.3499283

[14] S. H. Elazoumi, Results in Physics, 8, 16-25 (2018); https://doi.org/10.1016/j.rinp.2017.11.010

[15] N. F. Mott and E. A. Davis, Philosophical Magazine, 22(179), 903-922 (1970); https://doi.org/10.1080/14786437008228147

[16] Y. C. Ratnakaram, R. P. Sreekanth Chakradhar, K. P. Ramesh, J. L. Rao, and J. Ramakrishna, Journal of Materials Science, 38(4), 833-841 (2003); https://doi.org/10.1023/A:1021821317428

[17] V. Dimitrov and S. Sakka, Journal of Applied Physics., 79(4), 1741-1745 (1996); https://doi.org/10.1063/1.360963

[18] P. Naresh, D. Srinivasu, N. Narsimlu, Ch. Srinivas, B. Kavitha, Uday Deshpandhe, and K. Siva Kumar, in AIP Conference Proceedings, 1953l (2018)

[19] M. R. S. Nasuha, H. Azhan, W. A. W. Razali, L. Hasnimulyati, and Y. Norihan, Journal of Materials Science: Materials in Electronics, 32(18), 22890-22897 (2021); https://doi.org/10.1007/s10854-021-06766-w

[20] N. Baizura and A. K. Yahya, Journal of Non-Crystalline Solids, 357(15), 2810-2815 (2011); https://doi.org/10.1016/j.jnoncrysol.2011.03.003

[21] X. Zhang, Q. Chen, and S. Zhang, Molecules, 26(15) (2021);

https://doi.org/10.3390/molecules26154455
[22] P. Vani, G. Vinitha, K. A. Naseer, K. Marimuthu, M. Durairaj, T. C. Sabari Girisun, and N. Manikandan, Journal of Materials Science: Materials in Electronics, 32(18), 23030-23046 (2021); https://doi.org/10.1007/s10854-021-06787-5
[23] M. Khanisanij and H. A. A. Sidek, Advances in Materials Science and Engineering, 2014, (2014); https://doi.org/10.1155/2014/452830
[24] L. Hasnimulyati, M. K. Halimah, A. Zakaria, S. A. Halim, M. Ishak, C. Eevon, Journal of Ovonic Research, 12(6), 291-299 (2016)
[25] N. Elkhoshkhany, H. M. Mohamed, and E. Sayed Yousef, Results in Physics., 13 (2019); https://doi.org/10.1016/j.rinp.2019.102222
[26] A. Muhammad Noorazlan, H. Mohamed Kamari, S. S. Zulkefly, and D. W. Mohamad, Journal of Nanomaterials, 2013, (2013); https://doi.org/10.1155/2013/940917
[27] P. Gayathri Pavani, K. Sadhana, and V. Chandra Mouli, Physica B: Condensed Matter, 406(6-7), 1242-1247 (2011); https://doi.org/10.1016/j.physb.2011.01.006
[28] Y. S. Rammah, A. A. Ali, R. El-Mallawany, and F. I. El-Agawany, Physica B: Condensed Matter, 583, (2020); https://doi.org/10.1016/j.physb.2020.412055
[29] C. Madhukar Reddy, B. Deva Prasad Raju, N. John Sushma, N. S. Dhoble, and S. J. Dhoble, Renewable and Sustainable Energy Reviews., 51, 566-584 (2015); https://doi.org/10.1016/j.rser.2015.06.025
[30] M.K. Halimah, L. Hasnimulyati, A. Zakaria, S.A. Halim, M. Ishak, A. Azuraida, Naif Muhammed Al-Hada, Materials Science and Engineering B: Solid-State Materials for Advanced Technology B, 226, 158-163 (2017); https://doi.org/10.1016/j.mseb.2017.09.010
[31] A. S. Asyikin, M. K. Halimah, A. A. Latif, M. F. Faznny, and S. N. Nazrin, Journal of Non-Crystalline Solids, 529, (2020); https://doi.org/10.1016/j.jnoncrysol.2019.119777
[32] Y.B. Saddeek, K.A. Alya, K.S. Shaaban, Atif Mossad Alid, Moteb M. Alqhtani, Ali M. Alshehri, M.A. Sayed, E.A. Abdel Wahab, Journal of Non-Crystalline Solids, 498, 82-88 (2018); https://doi.org/10.1016/j.jnoncrysol.2018.06.002
[33] F. Nawaz, M. R. Sahar, S. K. Ghoshal, A. Awang, and I. Ahmed, Physica B: Condensed Matter, 433(1), 89-95, 2014; https://doi.org/10.1016/j.physb.2013.09.021
[34] H. A. Elbatal, A. M. Abdelghany, and I. S. Ali, Journal of Non-Crystalline Solids, 358(4), 820-825 (2012); https://doi.org/10.1016/j.jnoncrysol.2011.12.069
[35] P. Vani, G. Vinitha, M. I. Sayyed, M. M. AlShammari, and N. Manikandan, Nuclear Engineering and Technology, 53(12), 4106-4113 (2021); https://doi.org/10.1016/j.net.2021.06.009
[36] L. Hasnimulyati, M. K. Halimah, A. Zakaria, S. A. Halim, M. Ishak, C. Eevon, Journal of Ovonic Research, 12(6), 291-299 (2016)
[37] M. F. Faznny, M. K. Halimah, and M. N. Azlan, Journal of Optoelectronic and Bionedical Materials, 8(2), 49-59 (2016)
[38] A. H. Khafagy, A. A. El-Adawy, A. A. Higazy, S. El-Rabaie, and A. S. Eid, Journal of Non-Crystalline Solids, 354(27), 3152-3158 (2008); https://doi.org/10.1016/j.jnoncrysol.2008.01.013
[39] A. M. Noorazlan, H. Mohamed Kamari, S. S. Zulkefly, and D. W. Mohamad, Journal of Nanomaterials., 2013, (2013)
[40] M. Altaf and M. A. Chaudhry, Journal of the Korean Physical Society, 36(5), 265-268 (2000).
[41] A. Amat, M. K. Halimah, and N. Ahmad, Advanced Materials Research, 1107, 426-431, (2015); https://doi.org/10.4028/www.scientific.net/AMR.1107.426
[42] N. Elkhoshkhany, S. Marzouk, M. El-Sherbiny, S. Yousri, M. S. Alqahtani, H. Algami, E. S, Yousef, Results in Physics, 24, (2021); https://doi.org/10.1016/j.rinp.2021.104202
[43] J. N. Ayuni, M. K. Halimah, Z. A. Talib, H. A. A. Sidek, W. M. Daud, A. W. Zaidan and A. M. Khamirul, IOP Conference Series: Materials Science and Engineering, 17(1), (2011)
[44] R. El-Mallawany, M. D. Abdalla, and I. A. Ahmed, Materials Chemistry and Physics., 109(2-3), 291-296 (2008)